Sensors & Diagnostics

Accepted Manuscript

This article can be cited before page numbers have been issued, to do this please use: B. Correia, D. Oliveira , G. Vulpe, A. P. M. Tavares, M. G. F. Ferreira Sales, A. Duarte, S. Sharma and F. Moreira, *Sens. Diagn.*, 2023, DOI: 10.1039/D3SD00022B.

View Article Online
DOI: 10.1039/D3SD00022B

Cork based substrate coupled with artificial antibodies for point-of-care detection of pro-inflammatory cytokine biomarker

Bárbara Correia,[a#] Daniela Oliveira [a#], Georgeta Vulpe [b], Ana P.M. Tavares [c], M. Goreti F. Sales [c], Abel J. Duarte[d,e], Sanjiv Sharma [b*] and Felismina T.C. Moreira [a*]

Affiliation:

[a] BioMark@ISEP-CEB/LABBELS, School of Engineering, Polytechnic of Porto, R. Dr. António Bernardino de Almeida, 431, 4249-015 Porto, Portugal

[b] Department of Biomedical Engineering, Faculty of Science and Engineering, Swansea University, Swansea SA1 8EN (UK)

[c] BioMark@UC-CEB/LABBELS, Faculty of Sciences and Technology, University of Coimbra, R. Sílvio Lima, Pólo II, 3030-790 Coimbra, Portugal

[d] REQUIMTE, School of Engineering, Polytechnic of Porto, Porto, R. Dr. António Bernardino de Almeida, 431, 4249-015 Porto, Portugal

[e] ICETA, School of Engineering, Polytechnic of Porto, Porto, R. Dr. António Bernardino de Almeida, 431, 4249-015 Porto, Portugal

* *To whom correspondence should be addressed:*
Sanjiv Sharma email: sanjiv.sharma@swansea.ac.uk & Felismina Moreira email: ftm@isep.ipp.pt

View Article Online
DOI: 10.1039/D3SD00022B

Abstract

Whilst the single use point of care testing (PoCT) devices has transformed healthcare globally, there are major concerns over their environmental consequences. These concerns could be addressed employing devices made of environmentally friendly material. Herein, we report on the use of cork based PoCT device. Cork is known to be fully biodegradable and easily recycled without producing toxic residues. We report on how cork-based substrate coupled with a molecularly imprinted polymer (MIP) that serves as an "artificial antibody" can be used for point-of-care testing of the pro-inflammatory biomarker interleukin 6 (IL-6). The featured PoCT device has an electrochemical transducer that provides the desired clinical dynamic range for blood and can measure concentrations as low as 1 pg/mL, indicating its usefulness in point of care measurements for monitoring pathological disorders, worldwide. In addition, it has a huge environmental impact as it can reduce the waste generated by other polymeric/ceramic carriers used for the same purpose.

View Article Online
DOI: 10.1039/D3SD00022B

1.0 Introduction: The COVID-19 pandemic has led to an increased usage and demand for single use, disposable devices in the form of personal protective equipment and test-based lateral flow, intensifying pressure on an existing out-of-control problem of microplastic pollution [1]. More than eight million tons of pandemic-associated plastic waste have been generated globally, with more than 25,000 tons entering the global ocean. One of the main contributions to this problem was the use of rapid point-of-care testing (PoCT) diagnostic kits, to monitor and control the transmission of the virus between humans.

Although PoCT diagnostics play a vital role in both developed and developing countries, they employ substrates primarily based on affordability and mass production capability. The choice of synthetic substrates is based on their enhanced physicochemical properties, potential for personalised health monitoring, and ability to be customized for PoC diagnostics of cytokine biomarkers. [2,3] The material selection criteria include looking at the environment aspect. This includes looking at the impact of material and processing, the amount of waste generated, future legislation and the perception towards synthetic materials. It is therefore imperative to engineer sustainable healthcare devices based on natural, environmentally friendly materials.[4]

Electrochemical biosensors have attracted much attention due to their simplicity, suitability, low cost, and sensitivity in PoCT applications.[5] Several (bio)recognition elements have been used in sensing devices for the recognition of different analytes. Some rely on natural antibodies [6-10], others on synthetic reagents such as aptamers[11-13] or molecularly imprinted polymers (MIPs), also known as artificial antibodies. The use of MIP as bioreceptor, has become a powerful tool in the field of biosensors due to its advantages in terms of pH and temperature robustness, reusability, low cost, and stability.[14] They are fabricated in the presence of the target molecule, this is followed by the removal step of the imprinted target molecule to produce biomimetic cavities with complementary shape that allows efficient and selective recognition of structural features of small organic molecules and even large molecules such as proteins, viruses and bacteria[14].

Electrochemical PoCT devices employing MIP technology have shown to be a promising alternative to immunosensors. Several research papers have been described in the literature using MIP-based materials as a biological sensing layer for the detection of inflammatory biomarkers. IL-6 biosensors based on printing MIPs such as electropolymerised pyrrole [15], carboxylated pyrrole [16] and polydopamine [17] employing nanomaterial systems such as graphene, carbon nanotubes, metal-based nanoparticles and other adapters in commercial electrodes, have been reported for the relevant clinical range (1 - 200 pg/mL) with limit of detection below 1 pg/mL.

View Article Online
DOI: 10.1039/D3SD00022B

We report here, cork-based carbon printed electrodes imprinted with artificial antibodies for monitoring of cytokine biomarker IL-6. The replacement of plastic by cork is due to it being a natural, environmentally friendly material. Moreover, it biodegrades completely and can be easily recycled without producing toxic residues. “Artificial antibodies” employed as bioreceptors can be mass produced and therefore vital in manufacturing low cost PoCT devices. Owing to their enhanced physical, and chemical properties, as well as affordability and amenity to mass production, this combination of cork and artificial antibody has been employed to develop next-generation PoCT diagnostic devices with enhanced performances.

Herein, we demonstrate the capability of this combination towards developing PoC devices for a plethora of clinical applications involving real time monitoring of cytokines. Overexpression of interleukin 6 (IL-6) biomarkers can be found not only in blood but also saliva [18] and skin interstitial fluid (ISF)[19,20]. They are implicated in various medical conditions such as inflammatory diseases, infections, and different types of cancer including lung, colorectal, prostate, and breast cancers.

2. Experimental

2.1 Materials and methods

2.1.1Reagents and solutions. All solutions were prepared in ultrapure water with a conductivity of less than 0.1 µS/cm, purified by the Milli-Q system. Potassium hexacyanoferrate III ($K_3[Fe(CN)_6]$) and potassium hexacyanoferrate II ($K_4[Fe(CN)_6]$) trihydrate were obtained from Riedel-de Häen; potassium chloride (KCl) was obtained from Carlo Erba; phosphate buffered saline (PBS, 0.01 M, pH 7.4) solution was obtained from Panreac; sulfuric acid (H_2SO_4) was obtained from Sigma-Aldrich; 3-aminophenylboronic acid monohydrate 98% was obtained from Acros Organics; interleukin 6 (IL-6), 10 µg/mL, from Abcam. The carbon ink used herein was Sunchemical. The cork substrate used for this application was supplied by Amorim Cork Composites and chemically modified by the research team. This cork electrode modification consisted of introducing a film based on a commercial resin to make the substrate hydrophobic, and these substrates were characterised by SEM as reported in (Innovative screen-printed electrodes on cork composite substrates applied to sulfadiazine electrochemical sensing [21]. The waterproof layer was obtained by spinning a solution of a commercial resin at 1500 rpm for 60 seconds. The substrate was then dried overnight at 60 °C.

2.1.2 Instruments. Electrochemical measurements were performed in a Metrohm Autolab Potentiostat/Galvanostat equipped with an impedimetric module and controlled by the

View Article Online
DOI: 10.1039/D3SD00022B

software NOVA 2.1.5. Commercially available carbon ink-based screen printed electrodes (C-SPE) (Metrohm/DropSens, 110), carbon working and counter electrodes, and silver reference electrodes and electrical contacts were used. The switch box connecting the SPEs to the potentiostat was from BioTID, Portugal. The morphological and chemical properties of the sensor were analysed using spectroscopic methods such as Thermo Scientific's Raman spectroscopy technique (DXR 532 nm philtre) and scanning electron microscopy (SEM, Zeiss EVO LS25)

2.1.3. Fabrication of cork -SPE: The SPEs, used in this work were assembled by applying a commercial carbon ink on a cork substrate, as described by Tavares et al. [21]. The use of these greener sensors not only offers a more sustainable technology with less environmental impact than other carriers but is also cost-effective. MIP optimization was firstly performed by using commercial SPE electrodes from Metrohm DropSens (C-SPE) (A). The best conditions leading to reproducible results were defined, and the same analytical procedure was then applied to SPE electrodes with cork support (cork-SPE) (B) **(Figure S1, supplementary information).**

2.1.4.MIP Assembly: The protocol to modify the electrodes to MIP-biosensors comprises of three steps: electrode preparation (A), electropolymerisation (B), protein removal (C), this is followed by evaluation of the analytical performance of the sensor **(Figure 1).** First, 3-APBA was selected as monomer and prepared in PBS at pH 7.4. The protein imprinted film was prepared by electropolymerisation of 3-APBA 1 µg/mL in the presence of IL-6 protein, 10 µg/mL. The ratio in moles (number of molecules) is ~13:1 (monomer/template). Polymerization was achieved by cyclic voltammetry (CV), between -0.2 V and +1.0 V, at a scan rate of 0.02 V/s, for 15 cycles. The IL-6 protein was removed from the polymer matrix by incubating 0.5 M sulphuric acid solution on the working electrode for 1 hour at room temperature. It was then washed extensively with ultrapure water to remove the unreacted monomers and remove all IL-6 from the polymer matrix. In parallel, a non-imprinted polymer (NIP) was prepared. This material was prepared in a similar way to that described for the MIP, excluding, however, the template molecule from the procedure with replacement by the same volume of PBS, pH 7.4.

2.1.5. Analytical performance: Following the development of the MIP and NIP-based sensors, it is important to validate the analytical performance in terms of the ability to detect the IL-6 protein in the imprinted cavities. Therefore, the rebinding of IL-6 in MIP and NIP was tested to obtain a calibration curve expressing the relationship between the measured signal and the respective analyte concentration. The calibrations started with the incubation of IL-6 standard

View Article Online
DOI: 10.1039/D3SD00022B

solutions in increasing concentrations on the surface of the sensor layer over a period of 20 minutes.

All IL-6 standard solutions were prepared in a PBS buffer solution (pH 5). In accordance with the isoelectric point (PI) of IL-6, which has a value of 6.17 [16], the buffer solution used was more acidic to promote a solution with positive charges due to protonation of the amines present in the analyte and protonation of some acidic groups that are no longer negatively charged at this pH. Since the physiological value of IL-6 in a sample from a normal patient is 1.6 ± 0.8 pg/mL, 5 solutions were defined with standards of 1 pg/mL to 10000 pg/ml. These assays were repeated in a more realistic context, preparing standard solutions of IL-6 in Cormay serum, diluted one thousand-fold in PBS buffer (pH 5). Selectivity study by mixed solution assay using a fixed concentration of IL-6 (100 pg/mL) with glucose (0.7 mg/mL), urea (0.2 mg/mL) and BSA diluted one thousand-fold in PBS buffer, pH 5 (1 mg/mL). Incubation was at room temperature for 20 minutes. The respective interfering substances were prepared in buffer with pH 5.

2.1.6 Electrochemical assays: CV measurements were performed in the standard redox probe solutions containing 5 mM $K_3[Fe(CN)_6]$ and $K_4[Fe(CN)_6]$ prepared in 0.1 M KCl. At CV, the potential was scanned from -0.8 to +0.7 V at a scan rate of 50 mV/s. The electrochemical impedance spectroscopy (EIS) measurements were performed in a frequency range between 0.1 and 100 kHz with a scan of 50 frequencies and a sinusoidal potential from peak to peak with an amplitude of 0.01 V. A potential perturbation was used for the EIS. All EIS analyses were performed with an equivalent circuit, in this case a Randle circuit.

3. Results and discussion

3.1 Surface characterisation

3.1.1 *Electrochemical characterisation:* Molecular imprinting was carried out by electropolymerisation of the 3-APBA monomer using IL -6 as the target molecule by CV. The whole process consisted of two distinct phases: (1) protein imprinting by 3-APBA mixed with IL -6 (bulk solution), which formed a thin film on the surface of the working electrode; and (2) removal of IL -6 from the polymer matrix by treatment with sulfuric acid **(Figure 1).** All these phases resulted in changes in the electron transfer properties of the receptor surface and were evaluated by EIS and CV measurements.

The monomer used here has several advantages, including easy control of polymer thickness due to self-limiting growth and a simple regeneration process after use[23]. Furthermore, since IL -6 is a glycosylated cytokine, it is compatible with the boronic acid functional group in 3-

View Article Online
DOI: 10.1039/D3SD00022B

APBA. This is advantageous because boronic acid can covalently react with cis-diols to form five- or six-membered cyclic esters in an alkaline aqueous solution, which dissociate when the medium changes to an acidic pH. This remarkable chemistry makes boronic acids an interesting ligand for numerous applications in sensing, separation, and self-assembly [24].

In general, the CVs data obtained after MIP and NIP polymerization are consistent with the formation of an insulating layer after the 15 cycles of electropolymerisation at a scan rate of 0.02 V/s. For both materials, MIP and NIP, there was a significant decrease in current flow as a function of applied potential. In **(Figure S2-A1)** and **(Figure S2-A2),** a decrease in current and consequently a significant decrease in the height of the oxidation/reduction peaks was observed for both electrodes (C-SPE and cork) compared to the bare carbon electrodes. In addition, the decrease in current was more pronounced for the cork SPE

The EIS measurements support the data from CV. **(Figure 2S - B1 and B2**). After electropolymerisation of 3-APBA, an increase in charge transfer resistance (R_{ct}) from 1000 Ω to about 5000 Ω was observed. As can be seen in Figure S2 - B1 and B2, the R_{ct} of the MIP sensor is higher than NIP, which is built on commercial electrodes. This behaviour is expected when the protein causes an increase in R_{ct} due to its high molecular weight. However, an opposite behaviour was observed for the sensors fabricated on the cork-SPE. This behaviour was not expected since all steps are similar, and the only difference is the composition of the support material and the composition of the carbon ink. A possible explanation for this event is that the composition of the ink changes the structure of the film formed on the surface of the electrodes.

The final step of the imprinting process is the removal of the template removal from the polymer matrix. In this work, sulfuric acid was used as a release agent.[25] **Figure S2** shows the CVs and EIS results after template removal, and a higher effect was observed with cork-SPE **(A2 and B2).** Figure S2 shows the CVs and EIS results after template removal and a higher effect was observed for the cork-SPE **(A2 and B2).** Therefore, a slight increase in current was observed for the CVs technique, which was higher for the MIP built on cork SPE, with well-defined oxidation and reduction peaks. A plausible explanation is that the protein was removed from the polymeric matrix, and it could cause some cavities in the polymer, which facilities the electron transfer in the interface solution/electrode. The impedimetric tests agree with the CVs data, with a decrease in the impedance value compared to the electropolymerisation step. Thus, the results are consistent with expectations. For both NIP and MIP, there was a change in the response when the sulfuric acid chemically changed the

View Article Online
DOI: 10.1039/D3SD00022B

electrode surface. The difference between the removal step and the polymerization step was more pronounced for the MIPs.

3.1.2 Raman spectroscopy: The chemical modification of the working electrode for the different stages of MIP assembly and its control (NIP) was followed by Raman spectroscopy. The Raman spectra obtained are shown in **Figure 2** and have three peaks located at 1350, 1580 and 2700 cm^{-1} Raman shift. According to the literature, these peaks typically occur in carbon materials and are known as G, D, and 2D peaks, respectively.

Insert Figure 2 here (Raman spectra of the different immobilization stages of the biosensor)

The peaks are related to the hybridization of carbon atoms. The G peak represents the bonding vibrations of the sp^2 hybridization carbon atoms, indicating the C=C stretching, while the D peak expresses the sp^3 hybridization, indicating the defects in the carbon caused by chemical modification. Therefore, the intensity ratio between the D peak and the G peak is usually used to confirm the presence of a particular chemical modification in the carbon material.

The C-SPE bare exhibits an I_D/I_G ratio of 0.72. After electropolymerisation of MIP on it, an increase to 0.86 was observed, indicating that the carbon material was modified. The intensity ratio of MIP was higher than that of NIP, where it was 0.77, indicating that the difference in values was due to the presence of protein in the polymer matrix. Considering the results of the IL-6 removal step, where the ratio I_D/I_G decreased from 0.86 to 0.82, this suggests that the protein was successfully extracted from the polymer matrix. Moreover, NIP was subjected to the same conditions as MIP during the template removal process and showed almost no chemical change on its surface (I_D/I_G ratio of 0.78). This fact confirms the successful exit of the protein from the MIP assembly, while also confirming that the polymer network was unaffected by this removal stage. Overall, the Raman spectra confirmed the successful chemical change at each step associated with the assembly of MIP on the bare C-SPE surface.

3.1.3 Scanning electron microscope: The presence of imprinting sites could not be verified using SEM because electron microscopy is unable to distinguish with enough resolution such small cavities, making both the materials of MIP and NIP apparently similar. Still, **Figure 3** shows that the presence of the polymer on the C-SPE layer modified with MIP and NIP can be confirmed, as a thin film can be observed on the electrode surface. In addition, we did not observe any holes on the surfaces of MIP and NIP.

View Article Online
DOI: 10.1039/D3SD00022B

Insert Figure 3 here (SEM analysis for the commercially C-SPE, MIP and NIP materials)

3.2 Analytical response of the electrochemical biosensor: The analytical response of the MIP and NIP sensors was evaluated after optimizing the assembly parameters such as monomer concentration and pH. The calibration curve was generated by incubating different standards of protein IL-6 on the electrode surface. Solutions with increasing IL-6 concentrations from 1 pg/ml to 10000 pg/ml prepared in a buffer solution (PBS) with a pH of 5 were incubated for 20 min at 7 µl on the working electrode. After washing the electrode with ultrapure water, the electrochemical response between the different protein concentrations was then recorded for each sensor using a redox probe solution. This procedure was performed in parallel for the material NIP. The typical charge transfer resistance (R_{CT}) data obtained for MIP (A) and NIP (B) are shown in **Figure 4** for commercial electrodes. The electrochemical signal was then plotted against IL-6 concentration. The calibration curves were evaluated for the sensors of the commercial and homemade cork electrodes.

Insert Figure 4
EIS spectra of MIP and NIP sensors on commercially C-SPE and cork-SPE biosensors. MIP and NIP materials on commercial electrodes shown as A1 and B1, respectively. MIP and NIP materials on homemade cork electrodes are represented as A2 and B2, respectively. The measurements were performed with 5 mM $K_3[Fe(CN)_6]$ and $K_4[Fe(CN)_6]$ prepared in 0.1 M KCl solution.

Figure 4 shows that the MIP and NIP materials were able to elicit an electrochemical response as expected, with the highest sensitivity observed for the MIP materials. The gradual increase in hue **(**see Figure 5**),** from a light grey to a more intense orange for the MIPs, was proportional to the increase in incubated IL-6 concentration, which was more pronounced for the cork-SPEs.

On the other hand, in both NIPs, there was no linear response with the presence of increasing concentrations of IL-6. In the C-SPE, very short intervals between the different patterns were observed, with no response, as well as in the cork-SPE, there was a random response, especially at the concentration of 10 pg/mL and 1000 pg/mL, **Figure 5.** These results agreed with what was expected, since the NIP does not present cavities in the polymer matrix for the detection of IL-6, thereby also confirming that there is little non-specific interaction between the polymer layer and IL-6.

View Article Online
DOI: 10.1039/D3SD00022B

Insert Figure 5 here

Calibration curve of C-SPE electrodes left (1) and homemade cork-SPE right (2) with different concentration of IL-6 in PBS pH 5. The measurements were performed 5 mM K3[Fe(CN)6] and K4[Fe(CN)6] prepared in 0.1 M KCl solution.

Regarding the calibration of C-SPE and cork-SPE, it was found that only the protein-imprinted electrodes (MIP) showed a linear behaviour within 1 pg/mL to 10000 pg/mL **(Figure 5).** The material NIP showed a random behaviour. For both electrodes (C-SPE and cork-SPE), it was found that both MIPs had better analytical performance, with correlation coefficients of 0.9812 and 0.9865, respectively, and both values were significantly higher than those of NIPs (no linear behaviour). Comparing the analytical performance of the C-SPE and cork-SPE MIPs, it can be observed that the sensors prepared on cork had a higher slope 932[Ω/decade concentration)] compared to C-SPE, 704 [Ω/decade concentration] and a similar R^2, suggesting that the cork substrate could improve the performance of the sensors **(Figure 5).**

3.3. Application of biosensor for IL-6 detection in human serum: After calibrating the IL-6 biosensor in PBS, its performance was explored in a more realistic biofluid context. Thus, the same concentrations of standard solutions were prepared in Cormay serum (control material) diluted a thousand times in buffer solution at pH 5. **Figure S2** (Supplementary information) shows the EIS spectra of the calibration curves for MIP and NIP-based sensors in C-SPE electrodes **(A1 and B1)** and cork-SPE **(A2 and B2).**

According to **Figure S3** (Supplementary information)**,** a larger increase in the diameter of the Nyquist semicircle was observed for MIPs than for NIPs. An inversion of the slope of the calibration curves was observed for C-SPE electrodes. This could be attributed to possible interfering factors in the serum matrix that could interact with the ink and alter the net charge of the protein. In addition, the MIP and NIP sensors behaved oppositely in the cork-SPE (A2), and the resistance to charge transfer increased with increasing protein concentration. This behaviour was similar to that observed during calibrations in serum samples **(Figure S4)** (Supplementary information) .

Empirically, both MIPs were found to have better analytical performance for both C-SPE and cork-SPE, with correlation coefficients of 0.9952 and 0.9704, respectively, and both slopes were higher than those of NIPs. Moreover, (2) shows that the slope of MIP was 760 [Ω/(pg/mL)], which was higher than that of NIP, which was 582 [Ω/(pg/mL)]. These results show that the cork electrodes give consistent results and that, as expected, the calibration

View Article Online
DOI: 10.1039/D3SD00022B

curve in spiked serum has the same profile as the calibration in buffer, suggesting that serum does not have a strong influence on the MIP surface area.

3.4 Selectivity study: Selectivity tests were then performed to evaluate the ability of the sensor to distinguish IL-6 protein from other species present in biological fluids. In this way, fixed concentrations of IL-6 were incubated on the sensor surface along with various interfering species at concentrations corresponding to normal physiological conditions.

This study was performed with IL-6 (100 pg/mL), glucose (0.7 mg/mL), urea (0.2 mg/mL), and BSA diluted one thousand times in PBS buffer, pH 5 (1 mg/mL) **(Figure 6).** Incubation was performed for 20 minutes at room temperature and the respective interfering substances were prepared in buffer, pH 5. The lower the value of the percentage of interference, the lower the interference caused by the compound under study.

Insert Figure 6 here. (Selectivity study by mixed solutions method for the following possible interferents species: urea, glucose and BSA).

From the analysis of **Figure 6**, it is evident that each interfering substance slightly affects the electrochemical signal. The mean deviation (%) of the electrical signal produced by each interfering substance compared with the control (IL-6) was 8% for glucose, 9% for urea, and 15% for BSA. Observing the low percentages, it can be concluded from this study that there was no significant deviation in the interfering signals and therefore the sensor was found to be selective for the determination of IL-6 in synthetic human serum.

4. Conclusions

The development of selective electrochemical sensors is a recurrent approach and has recently evolved considerably. Their contribution in the medical field is the main objective of research, where it has been highlighted by monitoring the clinical condition of patients. In this work, an electrochemical sensor was developed by electrochemical polymerization with 3-APBA monomer to detect IL-6 protein and support the screening of this biomarker for inflammatory responses. However, it is important to note that this biomarker is non-specific and helps to complement an assay with specific biomarkers to support screening of the onset and progression of AD.

After all major optimizations, the analytical performance of both sensors was evaluated and good analytical responses were obtained with calibration curves in both PBS and Cormay serum, with correlation coefficients above 0.97 for the MIPs and lower values for the NIPs. To

View Article Online
DOI: 10.1039/D3SD00022B

complete this ideology, these two devices managed to obtain a linear response starting from 1 pg/mL, i.e., they have a detection limit below the physiological value of IL-6 in humans.

Nowadays, the use of natural products is widespread and used in all industries. Through the development of this work, it was possible to prove this ideology and show that it is feasible to combine the field of sensors with sustainability. The cork-based POCT biosensor was able to achieve better results than the conventional ceramic-based SPEs, moreover, they offer a decisive advantage of low cost and biodegradability of the PoCT device.

Conflicts of interest:

There are no conflicts to declare.

Author contributions: #BC and DO contributed equally to this manuscript towards investigation, methodology, validation and writing – original draft. GV and APT contributed in investigation (surface characterisation) and methodology. MGS, AJD and FTM contributed towards conceptualization, resources, and writing – review & editing. SS contributed towards methodology, investigation and writing – review & editing.

Acknowledgements:

The authors acknowledge funding through project 2IQBioneuro with the reference (0624_2IQBIONEURO_6_E), entitled, Promotion of an R&I network in biological chemistry for the diagnosis and treatment of neurological diseases, EP-INTERREG V Spain Portugal (POCTEP). Daniela O. acknowledge funding from Fundação para a Ciência e Tecnologia, I.P., through the PhD grant reference SFRH/BD/137832/2018. This work was also supported by Multi-year funding of European Union (FEDER funds through Compete) and National Funds (FCT/MCTES) through Project UID/QUI/50006/2019 and UIDB/04730/2020.

References:

1. J. D. Gallardo, G. L. Sullivan, M. Tokaryk, J. E. Russell, G. R. Davies, K. V. Johns, A. P. Hunter, T. M. Watson and S. Sarp, *Acs Es&T Water*, 2022, **2**, 527-538.
2. C. Liu, D. Chu, K. K. Zadeh, J. George, H. A. Young, G. Liu, Adv Sci (Weinh). 2021 Aug;8(15):2004433. doi: 10.1002/advs.202004433.
3. G. Liu, C. Jiang, X. Lin, Y. Yang, View (Beijing). 2021 Aug;2(4):20210003. doi: 10.1002/VIW.20210003.
4. M. G. Dobson, P. Galvin and D. E. Barton, *Expert Review of Molecular Diagnostics*, 2007, **7**, 359-370.
5. S. N. Topkaya, M. Azimzadeh and M. Ozsoz, *Electroanalysis*, 2016, **28**, 1402-1419.
6. R. Malhotra, V. Patel, J. P. Vaque, J. S. Gutkind and J. F. Rusling, *Analytical Chemistry*, 2010, **82**, 3118-3123.
7. Y. Lou, T. He, F. Jiang, J.J. Shi and J.J. Zhu, *Talanta*, 2014, **122**, 135-139.
8. J. J. Shi, T. T. He, F. Jiang, E. S. Abdel-Halim and J. J. Zhu, *Biosensors & Bioelectronics*, 2014, **55**, 51-56.
9. C. Russell, A. C. Ward, V. Vezza, P. Hoskisson, D. Alcorn, D. P. Steenson and D. K. Corrigan, *Biosensors & Bioelectronics*, 2019, **126**, 806-814.
10. E. B. Aydin, *Talanta*, 2020 Aug 1;215:120909. doi:10.1016/j.talanta.2020.120909.
11. M. Tertis, B. Ciui, M. Suciu, R. Sandulescu and C. Cristea, *Electrochimica Acta*, 2017, **258**, 1208-1218.
12. M. Tertis, P. I. Leva, D. Bogdan, M. Suciub, F. Graur and C. Cristea, *Biosens. Bioelectron. 137 (2019) 123-132*. doi: 10.1016/j.bios.2019.111410.
13. N. Chen, H. Yang, Q. Li, L. J. Song, S. C. B. Gopinath and D. Wu, *Biotechnol Appl Biochem. 2021 Dec;68(6):1479-1485. doi: 10.1002/bab.2068.*.
14. K. Haupt, A. V. Linares, M. Bompart and T. S. B. Bernadette, *Molecular Imprinting*, 2012, **325**, 1-28.
15. N. Ozcan, C. Karaman, N. Atar, O. Karaman and M. L. Yola, *2020 ECS J. Solid State Sci. Technol. 9 121010. doi: 10.1149/2162-8777/abd149*
16. M. d. L. Gonçalves, L. A. N. Truta, M. G. F. Sales and F. T. C. Moreira, *Analytical Letters*, 2021, 1-13.
17. Y. T. Yaman, O. A. Vural, G. Bolat and S. Abaci, *Bioelectrochemistry*, 2022, **145,** 108053. https://doi.org/10.1016/j.bioelechem.2022.108053.
18. J. C. Bloom, R. S. Fischer, A. Kim, C. Snell, G. M. Parkin, D. A. Granger, S. W. Granger and E. A. Thomas, *Int. J. Mol. Sci. 2020, 21(17), 6363; https://doi.org/10.3390/ijms21176363*.
19. X. Wang, M. R. Lennartz, D. J. Loegering and J. A. Stenken, *Cytokine*, 2008, **43**, 15-19.
20. B. P. Correa, D. Oliveira, S. Sharma, and F.T.C. Moreira, *Journal*, 2022, **7,43**, 39039–39044.
21. A. P. M. Tavares, M. H. de Sa and M. G. F. Sales, *Journal of Electroanalytical Chemistry*, 2021, **880, 114922**. http://dx.doi.org/10.1016/j.jelechem.2020.114922
22. P. S. Sharma, A. P. Le, F. D. Souza and W. Kutner, *Analytical and Bioanalytical Chemistry*, 2012, **402**, 3177-3204.
23. J. Zhang, X. T. Guo, J. P. Zhou, G. Z. Liu and S. Y. Zhang, *Materials Science & Engineering C-Materials for Biological Applications*, 2018, **91**, 696-704.

24. F. Frantzen, K. Grimsrud, D. E. Heggli and E. Sundrehagen, *Journal of Chromatography B-Biomedical Applications*, 1995, **670**, 37-45.
25. J. Erdossy, E. Kassa, A. Farkas and V. Horvath, *Analytical Methods*, 2017, **9**, 4496-4503.

View Article Online
DOI: 10.1039/D3SD00022B

View Article Online
DOI: 10.1039/D3SD00022B

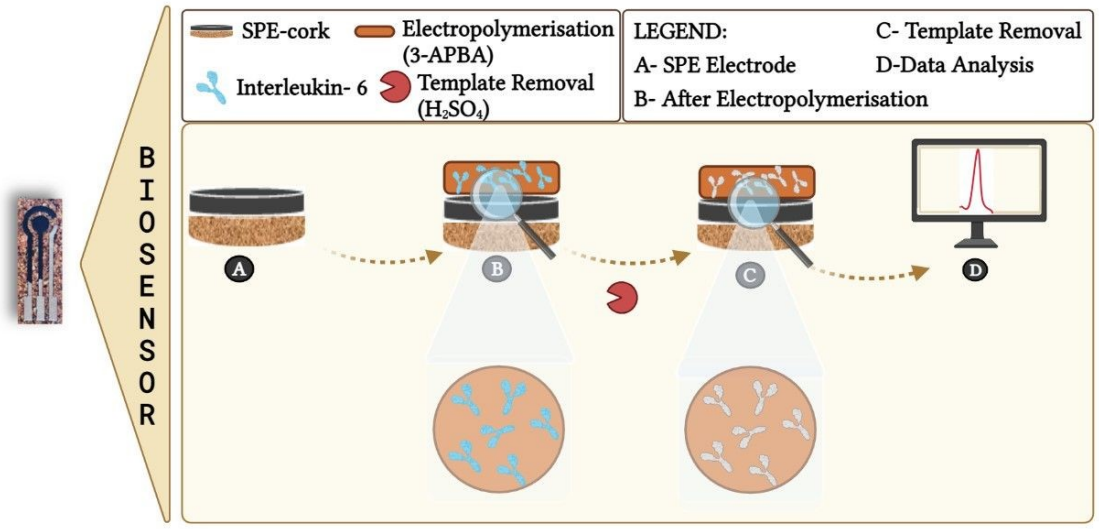

Figure 1 – Schematic of the construction of the sensor.

View Article Online
DOI: 10.1039/D3SD00022B

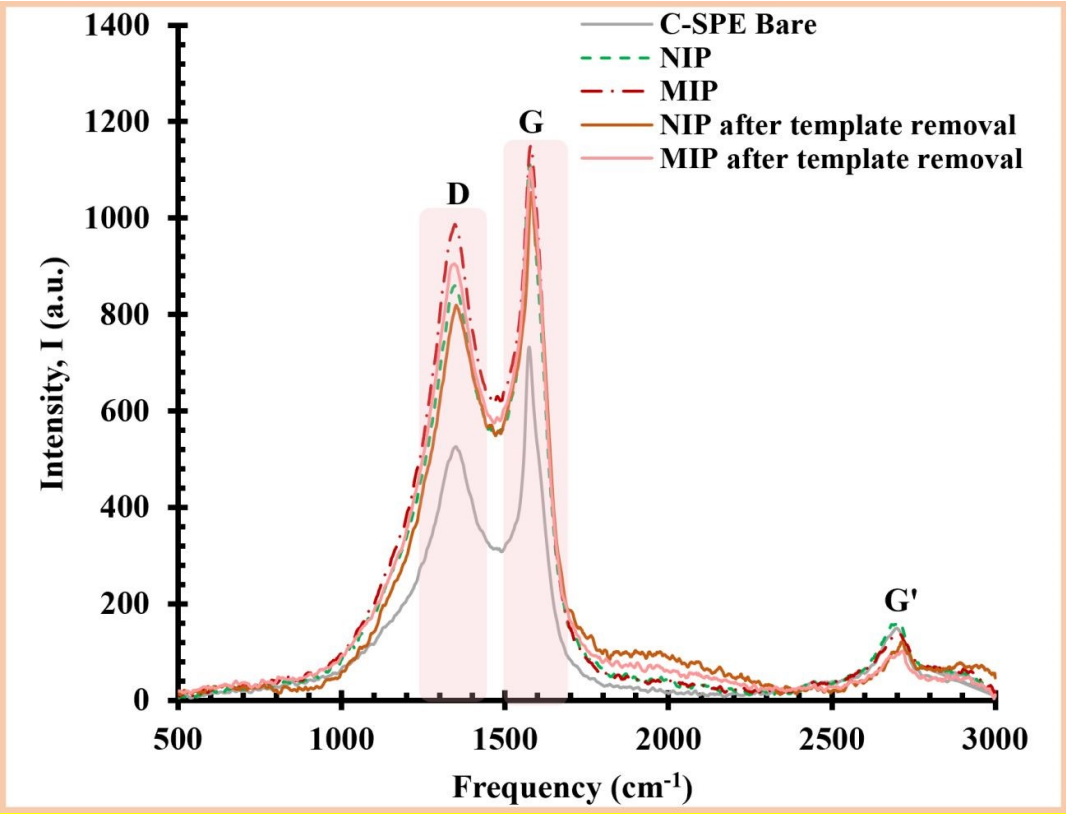

Figure2 - Raman spectra of the different immobilization stages of the biosensor.

View Article Online
DOI: 10.1039/D3SD00022B

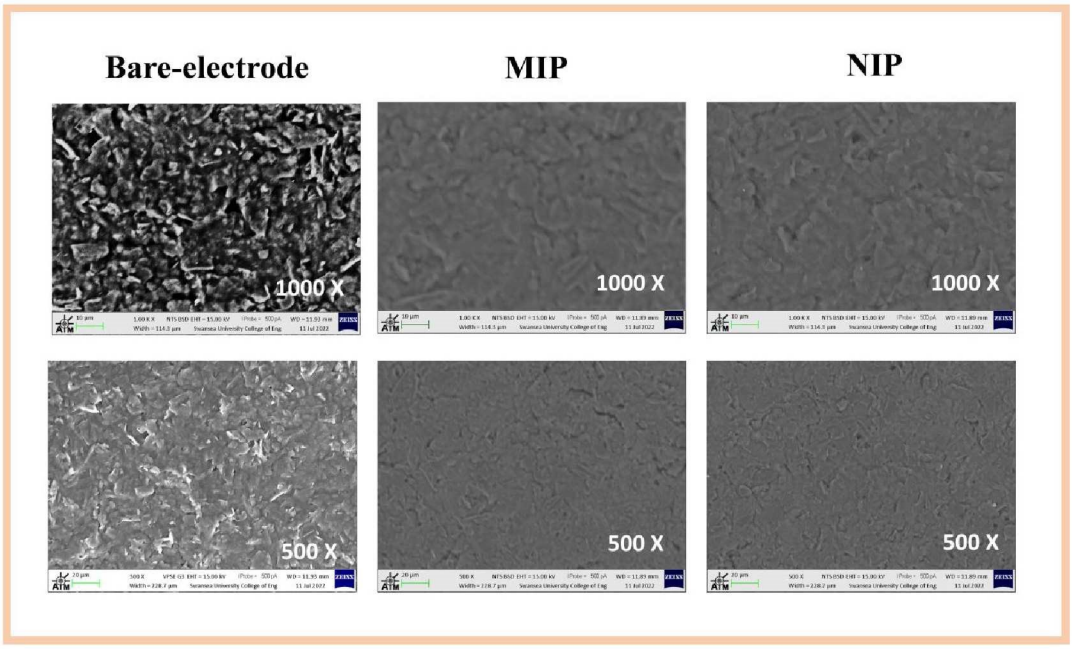

Figure 3- SEM analysis for the C-SPE, MIP and NIP materials.

View Article Online
DOI: 10.1039/D3SD00022B

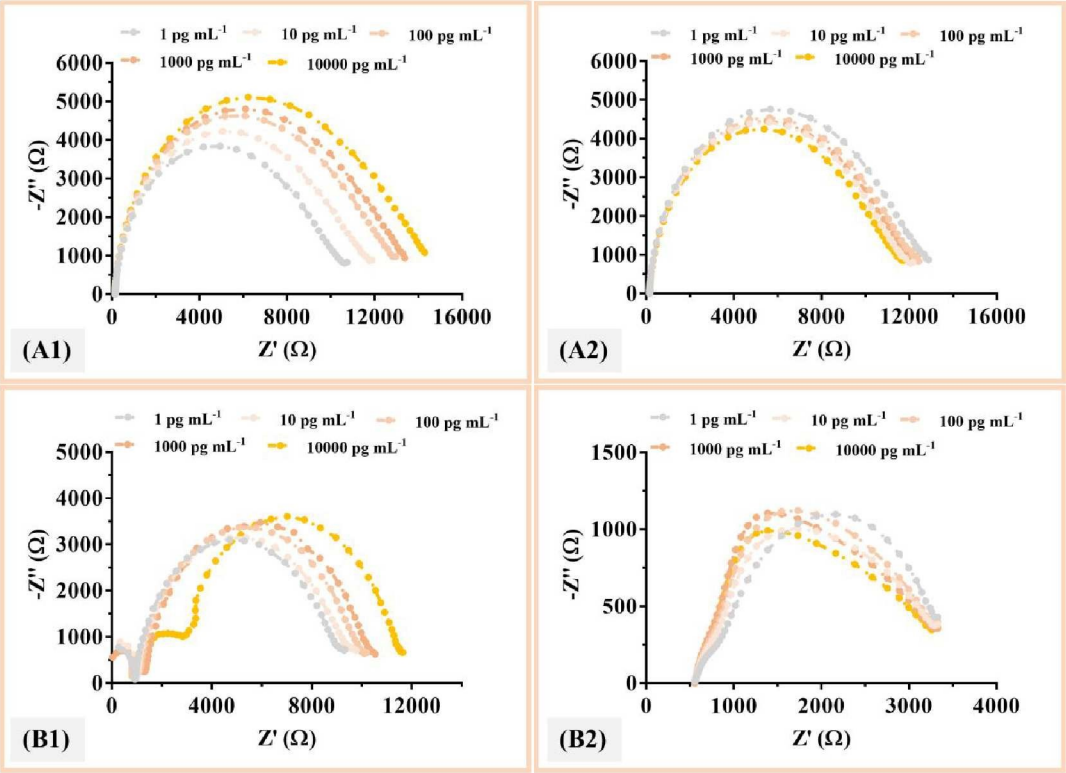

Figure 4 -EIS spectra of MIP and NIP sensors on commercially C-SPE and cork-SPE biosensors. MIP and NIP materials on commercial electrodes, (A1 e B1); MIP and NIP materials on homemade cork electrodes, (A2 and B2). The measurements were performed 5 mM $K_3[Fe(CN)_6]$ and $K_4[Fe(CN)^{6}]$ and prepared in 0.1 M KCl.

View Article Online
DOI: 10.1039/D3SD00022B

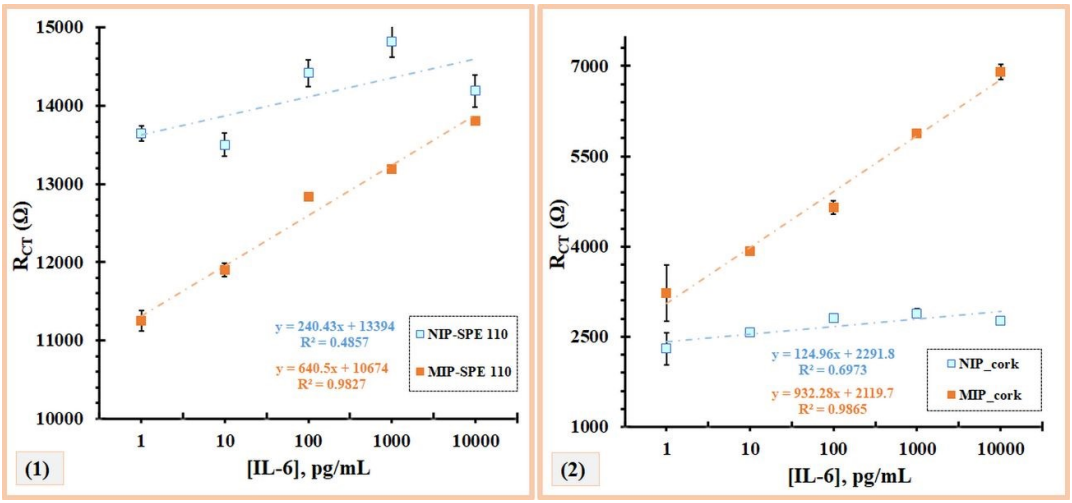

Figure 5 – Calibration curve of C-SPE electrodes (1) and homemade cork-SPE (2) with different concentration of IL-6 in PBS pH 5. The measurements were performed 5 mM $K_3[Fe(CN)_6]$ and $K_4[Fe(CN)_6]$ prepared in 0.1 M KCl.

View Article Online
DOI: 10.1039/D3SD00022B

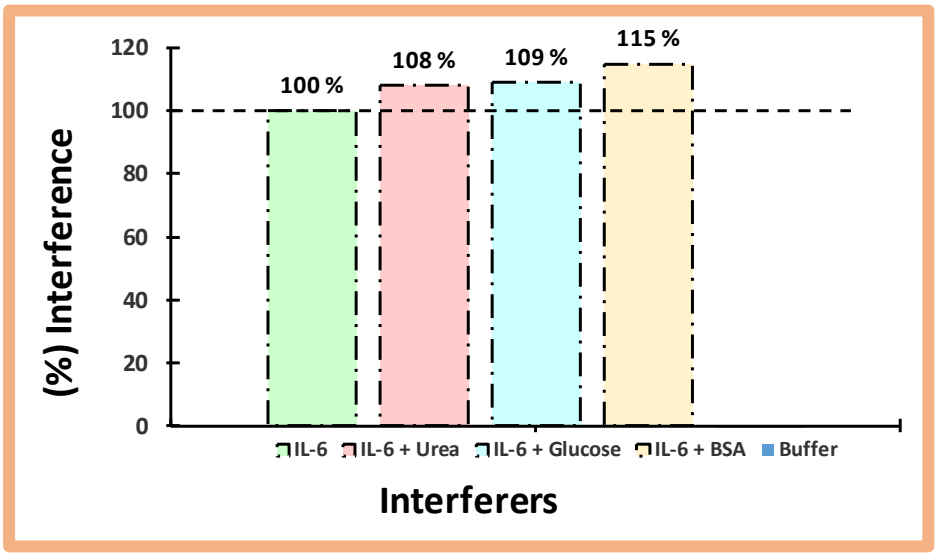

Figure 6 – Selectivity study by mixed solutions method for the following possible interferents species: urea, glucose and BSA.